Optics Letters

Tunable narrowband microwave photonic filter created by stimulated Brillouin scattering from a silicon nanowire

ALVARO CASAS-BEDOYA,* BLAIR MORRISON, MATTIA PAGANI, DAVID MARPAUNG, AND BENJAMIN J. EGGLETON

Center for Ultrahigh Bandwidth Devices for Optical Systems (CUDOS), Institute of Photonics and Optical Science (IPOS), School of Physics, University of Sydney, NSW 2006, Australia
**Corresponding author: casas@physics.usyd.edu.au*

Received 15 June 2015; revised 29 July 2015; accepted 10 August 2015; posted 17 August 2015 (Doc. ID 242936); published 31 August 2015

We demonstrate the first, to the best of our knowledge, functional signal processing device based on stimulated Brillouin scattering in a silicon nanowire. We use only 1 dB of on-chip stimulated Brillouin scattering gain to create an RF photonic notch filter with 48 dB of suppression, 98 MHz linewidth, and 6 GHz frequency tuning. This device has potential applications in on-chip microwave signal processing and establishes the foundation for the first CMOS-compatible high-performance RF photonic filter.

OCIS codes: (190.2640) Stimulated scattering, modulation, etc.; (190.4390) Nonlinear optics, integrated optics; (060.5625) Radio frequency photonics.

http://dx.doi.org/10.1364/OL.40.004154

Brillouin scattering is a light–sound interaction process that occurs when photons are scattered from a medium by induced acoustic waves [1]. Stimulated Brillouin scattering (SBS) is the strongest nonlinear process and manifests optically in ultranarrow resonances, which have been harnessed in optical fibers for slow light, sensing, and laser applications [2–6]. Recently, there has been strong interest in harnessing SBS in integrated platforms and unlocking functionalities unreachable by other means [7]. This has been demonstrated in various glasses such as silica or chalcogenides [8]. Although impressive results were achieved, these devices cannot be monolithically integrated with on-chip electro-optic modulators and photodetectors, which are readily available in silicon [9], to create a compact tunable filter.

Unfortunately, for the CMOS-compatible silicon-on-insulator (SOI) platform, SBS has been elusive. The low elastic mismatch between the silicon core and the silicon dioxide substrate result in weak acoustic confinement, preventing build-up of the SBS process. To remedy this, a recent demonstration employed a hybrid approach to remove the substrate while holding the nanowire with Si_3N_4 [10]. Although these results harnessed SBS in Si nanowires, they required an extra material and fabrication step, increasing overall complexity.

A recent breakthrough achieved forward propagating SBS (FSBS) in a silicon nanowire [11] by partially releasing the nanowire from its substrate. Here, they showed that SBS is enhanced at the nanoscale by radiation pressure contributions [11–13] and verified that electrostriction (a material property) in combination with radiation pressure (a geometrical property) increases the SBS gain. The amount of SBS gain that was reported, including this geometrical enhancement and novel fabrication methodology, was limited to around 4 dB [11], which is hardly usable for conventional signal processing applications.

In this Letter we report the first, to the best of our knowledge, functional device for signal processing based on SBS from a silicon nanowire. We employ a novel cancellation technique [14–16] to harness this modest SBS gain in silicon, creating a high-performance microwave photonic notch filter. We use only 0.98 dB of on-chip SBS gain to create a cancellation microwave photonic notch filter with 48 dB of suppression, 98 MHz linewidth, and 6 GHz frequency tuning. This demonstration establishes the path toward monolithic integration of high-performance SBS microwave photonic filters in a CMOS-compatible platform such as SOI.

Figure 1 summarizes the RF cancellation technique and working principle of the narrowband microwave photonic filter created by SBS. Initially reported in [15], the technique uses heterodyne photodetection to generate two RF mixing products between an optical carrier (ω_m) and two modulation sidebands. These two mixing products, having the same frequency, interfere. Destructive interference, however, occurs only at the frequency (ω_{RF}) where the optical sidebands have the same amplitude (A) and are in antiphase ($\varphi_2 - \varphi_1 = \pm\pi$). This particular amplitude/phase relationship between the sidebands is achieved through SBS ($\Omega_{SBSGain}$) on one of the sidebands. Therefore, in a frequency range equal to the SBS linewidth, the RF mixing products interfere destructively, resulting in a very narrowband, high-suppression electrical notch response. The center frequency of this notch response can be tuned simply by changing the position of the SBS resonance on the optical sideband, i.e., tuning the SBS pump wavelength (ω_p).

0146-9592/15/174154-04$15/0$15.00

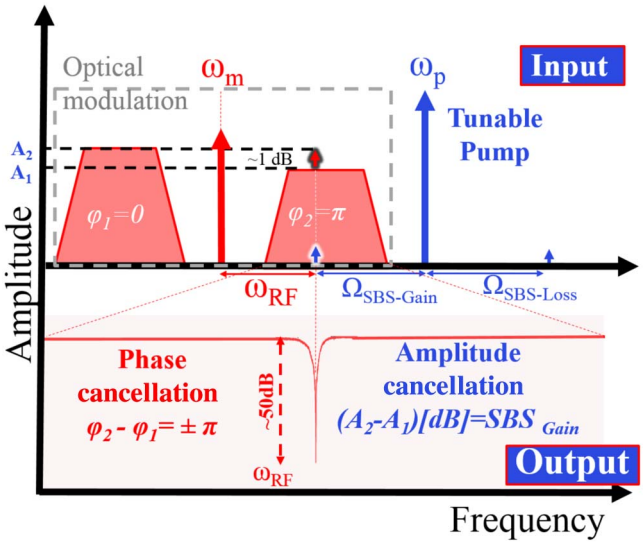

Fig. 1. Radio frequency cancellation technique and working principle of the tunable narrowband microwave photonic filter created by SBS.

The silicon nanowire was fabricated at IMEC through ePIXfab. The nanowires were immersed in 10% diluted hydrofluoric acid with an etching rate of 40 nm/min for 5.2 min to partially release them from the silica substrate. This created a 1.25 cm silicon nanowire with a cross section of 220 by 480 nm which was supported by a silica pillar of 50 nm width (Fig. 2, top). As reported in [11], such a structure restricts the phonon leakage and guarantees high confinement of the optical and acoustic modes allowing an efficient SBS interaction.

We proceeded with the optical characterization of the structure. We coupled 1550 nm transverse-electric- (TE) polarized light using focus grating couplers [17] into the chip and measured 5.2 dB coupling loss. We used an optical frequency domain reflectometer (OFDR) [18] to study the losses of our nanowire. This methodology infers the time-domain response via a Fourier transform from a modulated backscatter signal and consequently allows accurate measurements of the length of the nanowire and propagation losses, as shown in Fig. 2(a). Here, the first reflection peak is observed 722 cm away from the source. This length corresponds to the total length of our optical fibers just before the chip. The second reflected peak is observed 2.5 cm apart from this first reflection. This value corresponds to twice the length (L) of the nanowire as light is being reflected from the second grating coupler. Propagation losses (α) are also obtained with this technique by simply measuring the slope between both grating couplers reflections. This leads to $\alpha = 2.06$ dB/cm and thus an effective length of $L_{\text{eff}} = (1 - \exp(-\alpha \cdot L))/\alpha = 0.94$ cm.

We then measured the SBS gain response of the structure. With 30 mW of coupled pump power, we achieved a 0.98 dB of FSBS gain, which was the highest gain we measured in our structure. The measured Stokes and anti-Stokes have a Lorentzian profile at $\Omega/2\pi = 8.73$ GHz and are combined and plotted in Fig. 2(b). The calculated linewidth was fitted with a Lorentzian curve (red solid line) and calculated to be $\Gamma/2\pi = 98$ MHz. This leads to a quality factor of $Q_m = 89.09$ and a phonon life time $\tau = 1/\Gamma = 1.6$ ns.

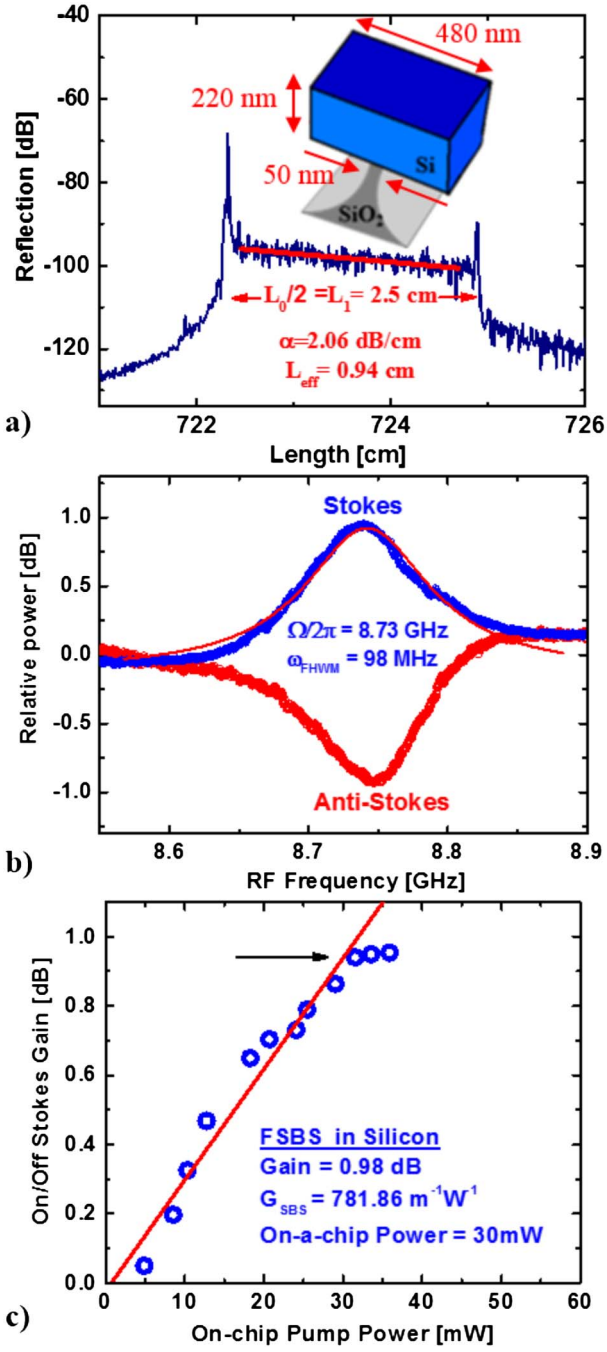

Fig. 2. (a) Optical frequency domain reflectometer measurement of a 1.25 cm silicon nanowire. The top of (a) shows a schematic representation of a partially suspended silicon nanowire. Note that during this work, we achieved a 50 nm pillar width. (b) Measured Stokes (blue) and anti-Stokes (red) FSBS frequencies. (c) Maximum Brillouin gain versus input pump power. The arrow indicates the SBS gain saturation at 30 mW due to nonlinear absorption. The red solid line is the fit performed to obtain the Brillouin gain coefficient (G_{SBS}).

We measured the maximum Stokes gain for different pump powers and plot them in Fig. 2(c). On resonance, the maximum Brillouin gain as function of pump power [P_p] is

$$I_s(L) = I_s(0) \cdot \exp(G_{SBS} \cdot P_p \cdot L_{eff}), \quad (1)$$

where $I_s(L)$ and $I_s(0)$ are the probe intensities, respectively, at the output and input of the device [8]. We use Eq. (1) to infer the SBS gain coefficient (G_{SBS}) below nonlinear absorption saturation. Using a linear fitting in Fig. 2(c), we obtain $G_{SBS} = 781.86\ m^{-1}\,W^{-1}$. This relatively low value is due to the phonon leakage through the postprocessed silica pillar [11]. However, we emphasize that creating a notch filter does not require an ultrahigh SBS gain or high pump powers. In fact, we show below how using a modest SBS gain and the elegant RF cancellation technique we create a CMOS-compatible cancellation filter.

The experimental setup employed to create our notch filter relies on forward SBS. Therefore, our measurement is based on transmission, not reflection as in [14], leading to a relatively simpler setup with less components. This approach is depicted schematically in Fig. 3. Here, using a dual-parallel Mach–Zehnder modulator (DPMZM), a CW optical carrier is modulated with the input RF signal. The DPMZM bias is set such that the modulation sidebands are π out-of-phase and with an amplitude mismatch of 1 dB. The modulated carrier and the SBS pump then copropagate along a 1.25 cm Si nanowire. The SBS pump frequency and power are set so that a FSBS 0.98 dB gain resonance is induced on the weaker sideband. In this way, only at the center of the SBS gain the modulation sidebands have equal amplitude, as well as being π out-of-phase. The SBS pump is then removed using a bandpass filter, which selects the modulated carrier and sends it to a photodetector (PD). Upon photodetection, the sidebands and the carrier mix, resulting in the output RF signal. However, only in the center of the SBS gain the sidebands reach equal amplitudes and the mixing products interfere destructively. This creates a high-suppression (>48 dB) notch response despite the low FSBS gain, as shown in Fig. 4(a).

The center frequency of the notch in the RF domain can be tuned simply by changing the frequency of the SBS pump. This tunability, in principle, makes the filter frequency immune to small changes in the Stokes frequencies that could arise from external factors such as temperature variations. As shown in Fig. 4(b), we were able to continuously tune the notch frequency over a 6 GHz range, while maintaining the notch suppression above 48 dB. The 6 GHz tuning range achieved during this experiment was limited by the bandpass filter. Here, we use a filter with a 3 dB bandwidth of 42 GHz centered at the optical carrier. As a consequence, the maximum accessible RF bandwidth was around 21 GHz, while the lower frequency was determined by the filter roll-off and its ability of efficiently removing the SBS pump frequency.

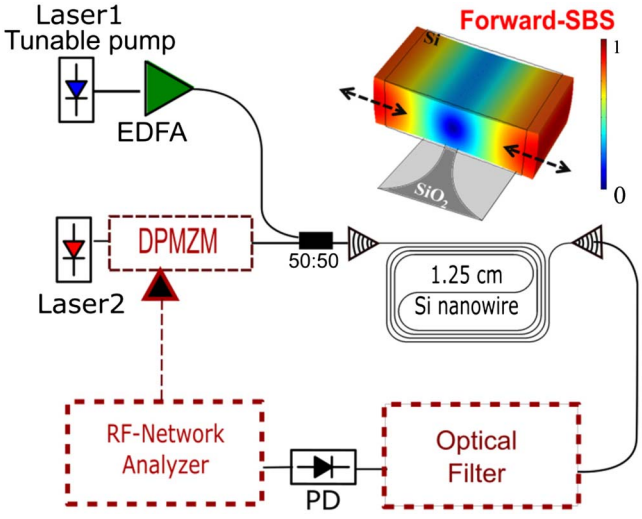

Fig. 3. Setup of the notch filter experiment. DPMZM, dual-parallel Mach–Zehnder modulator; PD, photodetector. The top right shows the simulated transversal acoustic displacement, or forward SBS, from a silicon nanowire.

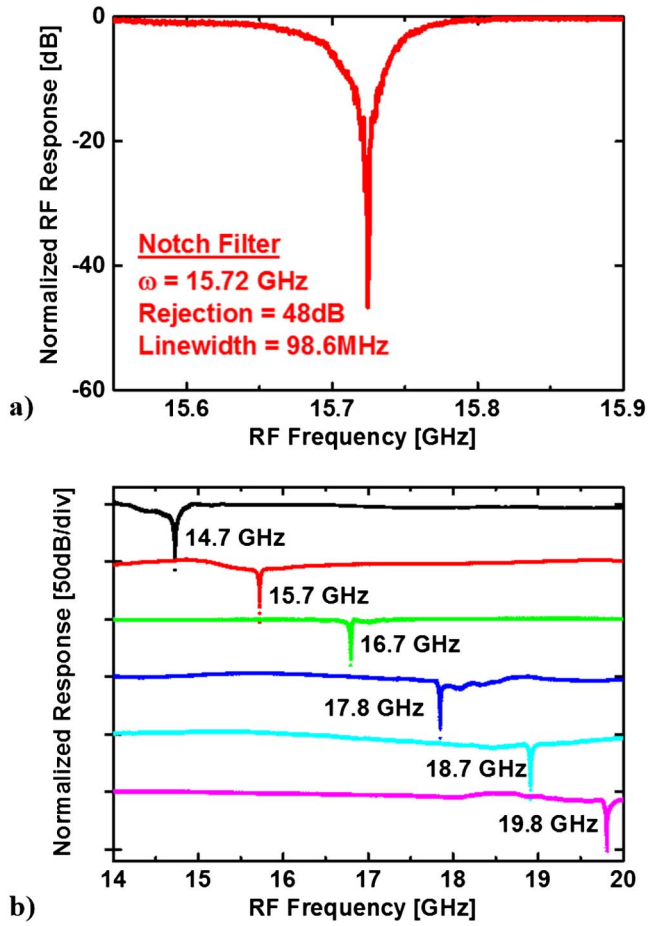

Fig. 4. (a) Measured RF notch filter response at 15.72 GHz. (b) Filter frequency tuning where the suppression was kept above 48 dB in all measurements.

To maintain an ultrahigh suppression over an entire RF tuning range is extremely challenging for conventional electronic-based RF notch filters as they exhibit limited resolution (gigahertz instead of megahertz linewidths) and are plagued by trade-offs between key parameters, such as frequency tuning range and suppression. For this reason, this demonstration represents the initial step toward the first, to the best of our knowledge, tunable integrated megahertz-resolution microwave photonic filter.

We demonstrated the first, to the best of our knowledge, functional device for signal processing based on SBS in silicon nanowires and establish the crucial first steps toward the creation of a high-resolution RF signal processor monolithically

integrated in a silicon chip, which will be a disruptive technology for next-generation radio-frequency systems with a wide range of applications. The filter is continuously tunable in the range of 14–20 GHz with a notch suppression of 48 dB and a 3 dB bandwidth of 98 MHz. We believe that combining our results with the already available library of modulators, tunable components, and photodetectors in SOI technologies will establish the foundation toward the first CMOS-compatible high-performance RF photonic filter.

Funding. Air Force Office of Scientific Research (AFOSR) (FA2386-14-1-4030); Australian Research Council (ARC) (CE110001018, DE150101535, FL120100029).

Acknowledgment. We acknowledge the fabrication of the silicon nanowires, which were done in the framework of the ePIXnet and the University of New South Wales (UNSW) node of the Australian National Fabrication Facility (ANFF) where the samples were etched.

REFERENCES

1. R. Boyd, *Nonlinear Optics* (Academic, 1992).
2. L. Thevenaz, Nat. Photonics **2**, 474 (2008).
3. X. Bao and L. Chen, Sensors **11**, 4152 (2011).
4. M. J. Damzen, V. I. Vlad, V. Babin, and A. Mocofanescu, *Stimulated Brillouin Scattering Fundamentals and Applications* (IOP, 2003).
5. M. Lee, R. Pant, and M. A. Neifeld, Appl. Opt. **47**, 6404 (2008).
6. S. P. Smith, F. Zarinetchi, and S. Ezekiel, Opt. Lett. **16**, 393 (1991).
7. B. J. Eggleton, C. G. Poulton, and R. Pant, Adv. Opt. Photon. **5**, 536 (2013).
8. R. Pant, C. G. Poulton, D.-Y. Choi, H. Mcfarlane, S. Hile, E. Li, L. Thevenaz, B. Luther-Davies, S. J. Madden, and B. J. Eggleton, Opt. Express **19**, 8285 (2011).
9. Y. Li, Q. Li, Y. Liu, M. Hochberg, and K. Bergman, "Integrated on-chip C-band optical spectrum analyzer using dual-ring resonators," in *CLEO*, San Jose, California (2015), paper SM1I.4.
10. H. Shin, W. Qiu, R. Jarecki, J. A. Cox, R. H. Olsson, A. Starbuck, Z. Wang, and P. T. Rakich, Nat. Commun. **4**, 1944 (2013).
11. R. Van Laer, B. Kuyken, D. Van Thourhout, and R. Baets, Nat. Photonics **16**, 1 (2015).
12. P. T. Rakich, P. Davids, and Z. Wang, Opt. Express **18**, 14439 (2010).
13. P. T. Rakich, C. Reinke, R. Camacho, P. Davids, and Z. Wang, Phys. Rev. X **2**, 011008 (2012).
14. D. Marpaung, B. Morrison, M. Pagani, R. Pant, D.-Y. Choi, B. Luther-Davies, S. Madden, and B. J. Eggleton, Optica **2**, 76 (2015).
15. D. Marpaung, B. Morrison, R. Pant, and B. J. Eggleton, Opt. Lett. **38**, 4300 (2013).
16. D. Marpaung, M. Pagani, B. Morrison, and B. Eggleton, J. Lightwave Technol. **32**, 3421 (2014).
17. F. Van Laere, T. Claes, J. Schrauwen, S. Scheerlinck, W. Bogaerts, D. Taillaert, L. O'Faolain, D. Van Thourhout, and R. Baets, IEEE Photon. Technol. Lett. **19**, 1919 (2007).
18. LUNA technologies, http://lunainc.com/.